Heralded Quantum Gate between Remote Quantum Memories

P. Maunz,[1,*] S. Olmschenk,[1] D. Hayes,[1] D. N. Matsukevich,[1] L.-M. Duan,[2] and C. Monroe[1]

[1]*Joint Quantum Institute, University of Maryland Department of Physics and National Institute of Standards and Technology, College Park, Maryland 20742, USA*

[2]*FOCUS Center and Department of Physics, University of Michigan, Ann Arbor, Michigan 48109, USA*

(Received 12 February 2009; published 25 June 2009)

We demonstrate a probabilistic entangling quantum gate between two distant trapped ytterbium ions. The gate is implemented between the hyperfine ''clock'' state atomic qubits and mediated by the interference of two emitted photons carrying frequency encoded qubits. Heralded by the coincidence detection of these two photons, the gate has an average output state fidelity of $89 \pm 2\%$. This entangling gate together with single qubit operations is sufficient to generate large entangled cluster states for scalable quantum computing.

DOI: 10.1103/PhysRevLett.102.250502 PACS numbers: 03.67.Bg, 03.67.Pp, 42.50.Ex

The conventional model of quantum computing, the quantum circuit model [1,2], consists of unitary quantum gate operations followed by measurements at the end of the computation process to read out the result. An equivalent model of quantum computation, which may prove easier to implement, is the ''one-way'' quantum computer [3–5], where a highly entangled state of a large collection of qubits is prepared and local operations and projective measurements complete the quantum computation.

Experiments with entangled photon states have demonstrated basic quantum operations [6,7] for one-way quantum computation. However, these experiments did not use quantum memories, and the photonic cluster states used as the resource for the computation are based on postselection and cannot easily be scaled [8]. In contrast, large entangled states of quantum memories can be generated using a photon-mediated quantum gate where the number of operations asymptotically scales linearly with the number of nodes [9–11]. The operation of the gate is heralded by the coincidence detection of two photons and thus can in principle be applied to a wide variety of quantum memories such as trapped ions, neutral atoms in cavities, atomic ensembles or quantum dots.

In this Letter, we demonstrate this probabilistic, heralded entangling gate for two ytterbium ions confined in two independent traps separated by 1 m. The gate is implemented between the long-lived hyperfine ''clock'' states and mediated by photons carrying frequency encoded qubits. Unlike the recent demonstration of teleportation between two ions [12], here we demonstrate and characterize the gate for arbitrary quantum states of both qubits, as required for scalable quantum computing. We perform the gate on a full set of input states for both qubits and measure an average fidelity of $89 \pm 2\%$. For the particular case that should result in the antisymmetric Bell state, we perform full tomography of the final state.

The gate has many favorable properties. The ions do not have to be localized to the Lamb-Dicke regime and the operation is not interferometrically sensitive to the optical path length difference. Because the qubits are encoded in the atomic hyperfine clock states and two well-separated photonic frequency states the system is highly insensitive to external influences. The operation of the gate between remote ions facilitates individual addressing for single qubit operations and measurement, and there is no need to shuttle ions. While the success probability of the gate in the current experiment is very small (2.2×10^{-8}), the scaling to large quantum networks is still efficient (polynomial instead of exponential) [9,10]; furthermore, it should be possible to significantly improve this rate for practical applications.

We trap two single $^{171}Yb^{+}$ atoms in two identically constructed Paul traps, located in independent vacuum chambers separated by approximately 1 m (Fig. 1). An ion typically remains in the trap for several weeks. Doppler-cooling by laser light slightly red detuned from the $^2S_{1/2} \leftrightarrow {}^2P_{1/2}$ transition at 369.5 nm localizes the ions to better than the diffraction limit of the imaging system but not to the Lamb-Dicke regime. With a probability of about 0.5%, the excited $^2P_{1/2}$ state decays to the metastable $^2D_{3/2}$ level. This level is depopulated with a laser near 935.2 nm to maintain efficient cooling and state detection. We apply an external magnetic field $B = 5.2$ Gauss to provide a quantization axis, break the degeneracy of the atomic states, and suppress coherent dark state trapping [13]. The atomic qubit is encoded in two $^2S_{1/2}$ ground-state hyperfine levels of the $^{171}Yb^{+}$ atom, with $|0\rangle := |F = 0, m_F = 0\rangle$ and $|1\rangle := |F = 1, m_F = 0\rangle$, which have a separation of 12.6 GHz [Fig. 2(a)]. Here F is the total angular momentum of the ion and m_F its projection along the quantization axis. These hyperfine clock states are, to first order, insensitive to the magnetic field and thus form an excellent quantum memory [14,15].

The remote gate protocol is shown schematically in Fig. 2. We first initialize each ion in $|0\rangle$ with a 1 μs pulse of light resonant with the $^2S_{1/2}(F = 1) \leftrightarrow {}^2P_{1/2}(F = 1)$ transition. Then we independently prepare each ion

Report Documentation Page

Form Approved
OMB No. 0704-0188

1. REPORT DATE	2. REPORT TYPE	3. DATES COVERED
FEB 2009		**00-00-2009 to 00-00-2009**

4. TITLE AND SUBTITLE	5a. CONTRACT NUMBER
Heralded Quantum Gate between Remote Quantum Memories	5b. GRANT NUMBER
	5c. PROGRAM ELEMENT NUMBER
6. AUTHOR(S)	5d. PROJECT NUMBER
	5e. TASK NUMBER
	5f. WORK UNIT NUMBER
7. PERFORMING ORGANIZATION NAME(S) AND ADDRESS(ES) **University of Maryland,Department of Physics,Joint Quantum Institute,College Park,MD,20742**	8. PERFORMING ORGANIZATION REPORT NUMBER
9. SPONSORING/MONITORING AGENCY NAME(S) AND ADDRESS(ES)	10. SPONSOR/MONITOR'S ACRONYM(S)
	11. SPONSOR/MONITOR'S REPORT NUMBER(S)

12. DISTRIBUTION/AVAILABILITY STATEMENT
Approved for public release; distribution unlimited

13. SUPPLEMENTARY NOTES

14. ABSTRACT

15. SUBJECT TERMS

16. SECURITY CLASSIFICATION OF:			17. LIMITATION OF ABSTRACT	18. NUMBER OF PAGES	19a. NAME OF RESPONSIBLE PERSON
a. REPORT **unclassified**	b. ABSTRACT **unclassified**	c. THIS PAGE **unclassified**	**Same as Report (SAR)**	**4**	

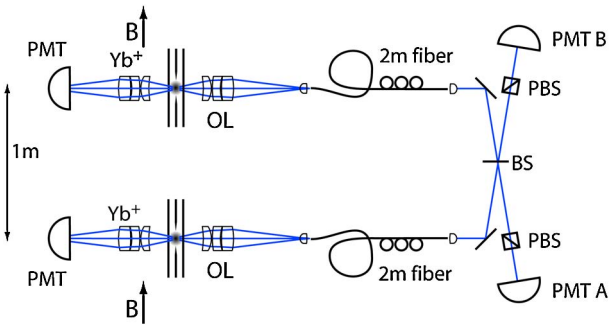

FIG. 1 (color online). The experimental apparatus. Two $^{171}Yb^{+}$ ions are trapped in identically constructed ion traps separated by 1 m. A magnetic field B is applied perpendicular to the excitation and observation axes to define the quantization axis. About 2% of the emitted light from each ion is collected by an imaging system (OL) with numerical aperture of about 0.3 and coupled into single-mode fibers. Polarization control paddles are used to adjust the fibers to maintain linear polarization. The output of these fibers is directed to interfere on a polarization-independent 50% beam splitter (BS). Polarizers (PBS) transmit only the π-polarized light from the ions. The photons are detected by single-photon counting photomultiplier tubes (PMT A and PMT B). Detection of the atomic state is done independently for the two traps with dedicated photomultiplier tubes (PMTs).

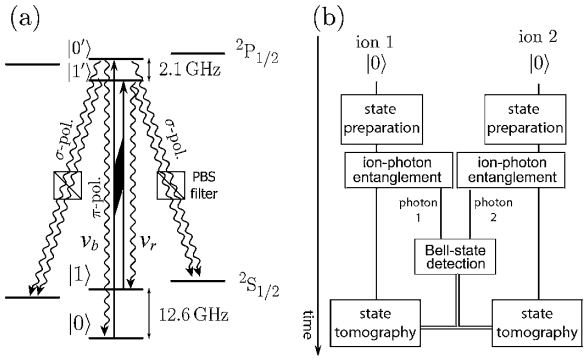

FIG. 2. (a) Level and excitation scheme. The qubit is encoded in the $^2S_{1/2}$ hyperfine clock states of the $^{171}Yb^{+}$ ion and is coherently excited to the $^2P_{1/2}$ hyperfine excited states by a pulse from an ultrafast laser with a wavelength centered near 369.5 nm. Upon spontaneous emission of a π-polarized photon, the frequency state of the photon is entangled with the qubit state of the atom. A polarizer (PBS) blocks photons from different decay channels. (b) Gate operation scheme. After initialization in $|0\rangle$, ion 1 and 2 are prepared in the input states $|\Psi_a\rangle_1$ and $|\Psi_a\rangle_2$, respectively. The frequency of each spontaneously emitted π-polarized photon is entangled with the state of the respective ion. If these two photons are detected in the antisymmetric Bell state, the quantum state of the two ions is projected on the state $|\Psi_{aa}\rangle \propto Z_1(I - Z_1Z_2)|\Psi_a\rangle_1|\Psi_a\rangle_2$. Here Z_i is the Pauli-z operator acting on ion i.

$(i = 1, 2)$ in any desired superposition state $|\Psi_a\rangle_i = \alpha_i|0\rangle_i + \beta_i|1\rangle_i$ by applying a resonant microwave pulse with controlled phase and duration (0–16 μs). Next, we use an ultrafast π-polarized resonant laser pulse to simultaneously transfer the superposition from the ground state qubit states to the $^2P_{1/2}$ hyperfine states $|0'\rangle := |F' = 1, m'_F = 0\rangle$ and $|1'\rangle := |F' = 0, m'_F = 0\rangle$ of each ion with near-unit efficiency. For π-polarized light the dipole selection rules allow only the transitions $|0\rangle \leftrightarrow |0'\rangle$ and $|1\rangle \leftrightarrow |1'\rangle$ which have equal transition strength. The two transitions are well-resolved, as their center frequencies are separated by $\Delta\nu = 14.7$ GHz, while the natural linewidth of the excited state is only about 20 MHz. The bandwidth of the 1 ps pulse of about 300 GHz is broad compared to $\Delta\nu$ but small compared to the fine structure splitting in Yb^{+} of about 100 THz, allowing both transitions to be driven equally while the population of the excited $^2P_{3/2}$ state remains vanishingly small. Consequently, the qubit can be transferred coherently from the $^2S_{1/2}$ ground state to the excited $^2P_{1/2}$ state [16].

Following excitation, each ion will emit a single photon. Upon emission of a π-polarized 369.5 nm photon, the frequency mode of the emitted photon and the state of the ion are in the entangled state $|\Psi_{ap}\rangle_i = \alpha_i|0\rangle_i|\nu_b\rangle_i + \beta_i|1\rangle_i|\nu_r\rangle_i$, where $|\nu_b\rangle$ and $|\nu_r\rangle$ are the two possible frequency states of the emitted photon. The state of the total system is $|\Psi_{apap}\rangle = |\Psi_{ap}\rangle_1 \otimes |\Psi_{ap}\rangle_2$. For each ion, emitted photons are coupled into a single-mode fiber. The output of the fiber from each ion is directed to interfere on a polarization-independent 50% beam splitter. Each output of the beam splitter is directed through a linear polarizer and detected with a single-photon counting photomultiplier tube. To ensure high contrast interference of the two photons from different ions, the photons must be indistinguishable. To this end, we first minimize the micromotion of the ions to prevent modulation of the emission frequency. Second, the geometrical modes from the two fibers are matched to better than 98% as characterized with laser light. Third, the emitted photons are matched in their arrival time at the beam splitter to better than 100 ps. As a consequence of the quantum interference [17–19], two photons, each in a superposition of two frequency modes, can only emerge from different output ports of the beam splitter if they are in the antisymmetric state $|\psi^-_{pp}\rangle = (|\nu_b\rangle_1|\nu_r\rangle_2 - |\nu_r\rangle_1|\nu_b\rangle_2)/\sqrt{2}$. Upon coincidence detection of two photons at the two output ports of the beam splitter, the ions are projected onto the state

$$|\Psi_{aa}\rangle = \frac{1}{\sqrt{2P_{|\psi^-\rangle}}}(\alpha_1\beta_2|0\rangle_1|1\rangle_2 - \beta_1\alpha_2|1\rangle_1|0\rangle_2) = \frac{1}{\sqrt{2P_{|\psi^-\rangle}}}\frac{Z_1(I - Z_1Z_2)}{2}|\Psi_a\rangle_1|\Psi_a\rangle_2, \quad (1)$$

where Z is the Pauli-z operator and $P_{|\psi^-\rangle} = (\alpha_1^2\beta_2^2 + \beta_1^2\alpha_2^2)/2$ is the probability to find the photons in the antisymmetric Bell state. Thus the coincidence detection of two photons heralds the operation of the remote two-ion

quantum gate $Z_1(I - Z_1Z_2)$. In contrast to a simple entanglement process [20], the final state depends on the initial states of both ions. This property of the entangling gate is essential for the efficient generation of cluster states of more than two ions. Being a projection or measurement gate, this process is not unitary. Indeed, for the input states $|0\rangle_1|0\rangle_2$ and $|1\rangle_1|1\rangle_2$ a heralding event should never occur. This would be calamitous in the circuit model, however, in the protocol to generate cluster states, the input qubits are by design in a superposition of the two qubit states. In this case, the protocol succeeds with a nonvanishing probability and scales favorably [10].

To verify the operation of the gate we first characterize the generation of the maximally entangled antisymmetric Bell state $|\Psi_{aa}\rangle = (|0\rangle|1\rangle - |1\rangle|0\rangle)/\sqrt{2}$ by full state tomography. Both ions are prepared in $|\Psi_a\rangle_i = (|0\rangle_i + |1\rangle_i)/\sqrt{2}$ and operated on by the gate. We then measure the state of each ion in three mutually unbiased bases. Detection of the quantum state of each ion in the x (y) bases is done by first applying a resonant microwave $\pi/2$ pulse with a relative phase of 0 ($\pi/2$) with respect to the initial microwave pulse. Standard fluorescence detection is then used to determine the quantum state of the ion; the ion scatters light if found in state $|1\rangle$, while it remains dark if found in $|0\rangle$ [15]. Consequently, we get an answer in every attempt to measure the state and this answer is correct with more than 98% probability. The density matrix (Fig. 3) is obtained using a maximum likelihood algorithm [21]. From this density matrix we calculate the entangled state fidelity $F = 0.87(2)$, the concurrence $C = 0.77(4)$ and the entanglement of formation $E_F = 0.69(6)$. The entanglement of this state is considerably higher than in our previous experiments [22,23] due to technical improvements and the superior coherence properties of the photonic frequency and atomic clock state qubits.

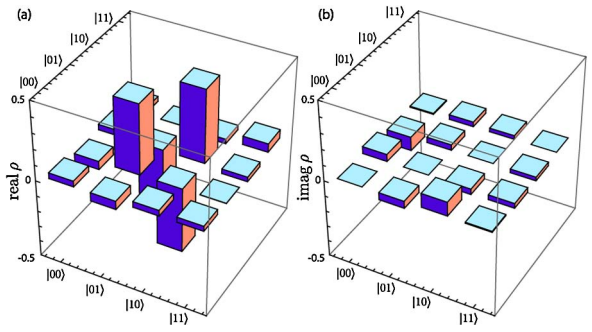

FIG. 3 (color online). State Tomography of the final state $|\Psi_{aa}\rangle \propto Z_1(I - Z_1Z_2)(|0 + 1\rangle_1|0 + 1\rangle_2)$. Real (a) and imaginary (b) part of the reconstructed density matrix. The fidelity of the expected output state $|0\rangle_1|1\rangle_2 - |1\rangle_1|0\rangle_2$ of the gate is $F = 0.87(2)$. The generated state has a concurrence of $C = 0.77(4)$ and an entanglement of formation of $E_F = 0.69(6)$. The density matrix is obtained with a maximum likelihood algorithm from 601 events measured in 9 different bases.

To characterize the functionality of the gate for arbitrary input states we measure the fidelity of the output state for a representative set of input states as shown in Table I and obtain an average fidelity of $\bar{F} = 0.89(2)$. We do not characterize the action of the gate on certain input states that differ only by global qubit rotations. Such states are identical to those considered up to an overall choice of basis, so the input states listed in Table I are representative of a full set of unbiased qubit bases.

The observed entanglement and average output state fidelity of the gate are consistent with known experimental imperfections. The primary error sources that reduce the fidelity are imperfect state detection (3%), geometrical mode mismatch on the beam splitter (6%), and detection of σ-polarized light due to the nonzero solid angle and misalignment of the magnetic field ($<2\%$). Micromotion at the rf-drive frequency of the ion trap, which alters the spectrum of the emitted photons and can degrade the quantum interference, is expected to contribute to the overall error less than 1%. Other error sources include imperfect state preparation, pulsed excitation to the wrong atomic state, dark counts of the PMT leading to false coincidence events, mismatch of the quantization and polarizer axes, and multiple excitation due to pulsed laser light leakage, and are each estimated to contribute much less than 1% to the overall error.

The entangling gate demonstrated here is heralded by a two-photon coincidence detection. Thus, the success probability is given by the square of the single photon detection probability times the probability to find two photons in the antisymmetric Bell state

$$P_{\text{gate}} = P_{|\psi^-\rangle}\left(p_\pi \frac{\Delta\Omega}{4\pi} T_{\text{fiber}} T_{\text{optics}} \eta\right)^2 \approx P_{|\psi^-\rangle} 8.5 \times 10^{-8}.$$

Here $p_\pi = 0.5$ is the probability that a collected 369.5 nm photon is π polarized, $\Delta\Omega/4\pi = 0.02$ is the collection solid angle, $T_{\text{fiber}} = 0.2$ is the coupling and transmission efficiency through the single-mode fiber, $T_{\text{optics}} = 0.95$ is the transmission coefficient of the other optics, and $\eta = 0.15$ is the quantum efficiency of the photomultiplier tube. The probability to find two photons in the antisymmetric Bell state $P_{|\psi^-\rangle}$ is a function of the initial states with $0 \leq P_{|\psi^-\rangle} \leq 1/2$. The experiment was repeated at about 70 kHz leading to an average time of 11 min between events, longer than the 2.5 s coherence time measured in our setup [15] but on the order of the more than 12 min coherence time observed for the chosen qubit states [14].

To realize a large entangled cluster state, the average time per gate operation must be short compared to the qubit coherence time and the gate fidelity has to be sufficiently high to exceed the threshold value for fault tolerant quantum computation with cluster states [24]. The average gate time is limited by the repetition rate and, most importantly, the photon collection probability. Currently, photons are collected by a lens which only covers a small solid angle.

TABLE I. Results of the remote quantum gate process. Listed are the input and expected output states of the gate, the measurement performed to obtain the fidelity (overlap with the expected output state), the number of heralding events, and the measured and ideal probability for two photons to be in the antisymmetric Bell state. The success probability of the gate is $P_{\text{gate}} = P_{|\psi^-\rangle} \times 8.5 \times 10^{-8}$. Here, $p(|0\rangle|1\rangle)$ is the probability to measure state $|0\rangle|1\rangle$ and the parity $\mathcal{P}_{xy}$ is the difference of the probabilities to find the two ions in the same state and in opposite states when ion 1, 2 is measured in the x, y basis, respectively. The other parity values are defined similarly. From these results we calculate the average gate fidelity $\bar{F} = 0.89(2)$.

Input state	Expected state	Measurement	Fidelity	Events	$P_{\|\psi^-\rangle}$ (meas.)	$P_{\|\psi^-\rangle}$(theo.)
$\|0+1\rangle \otimes \|0+1\rangle$	$\|0\rangle\|1\rangle - \|1\rangle\|0\rangle$	$\frac{1}{4}(1 - \mathcal{P}_{xx} - \mathcal{P}_{yy} - \mathcal{P}_{zz})$	0.89(2)	210	0.26(1)	1/4
$\|0+i1\rangle \otimes \|0+1\rangle$	$\|0\rangle\|1\rangle - i\|1\rangle\|0\rangle$	$\frac{1}{4}(1 - \mathcal{P}_{xy} + \mathcal{P}_{yx} - \mathcal{P}_{zz})$	0.86(2)	179	0.26(1)	1/4
$\|0-1\rangle \otimes \|0+1\rangle$	$\|0\rangle\|1\rangle + \|1\rangle\|0\rangle$	$\frac{1}{4}(1 + \mathcal{P}_{xx} + \mathcal{P}_{yy} - \mathcal{P}_{zz})$	0.85(1)	178	0.22(2)	1/4
$\|0-i1\rangle \otimes \|0+1\rangle$	$\|0\rangle\|1\rangle + i\|1\rangle\|0\rangle$	$\frac{1}{4}(1 + \mathcal{P}_{xy} - \mathcal{P}_{yx} - \mathcal{P}_{zz})$	0.81(2)	188	0.27(2)	1/4
$\|0+1\rangle \otimes \|1\rangle$	$\|0\rangle \otimes \|1\rangle$	$p(\|0\rangle\|1\rangle)$	0.86(5)	42	0.24(4)	1/4
$\|0\rangle \otimes \|0+1\rangle$	$\|0\rangle \otimes \|1\rangle$	$p(\|0\rangle\|1\rangle)$	0.91(4)	52	0.20(3)	1/4
$\|0\rangle \otimes \|1\rangle$	$\|0\rangle \otimes \|1\rangle$	$p(\|0\rangle\|1\rangle)$	0.98(2)	48	0.39(6)	1/2
$\|0\rangle \otimes \|0\rangle$	0			65	0.04(1)	0

The solid angle can be significantly increased by using parabolic mirrors [25] or microstructured lenses [26]. Furthermore, the spontaneous emission into free space could be replaced by the induced emission into the small mode volume of a high finesse cavity [27,28] which can reach near-unit efficiency. Even though the free spectral range of the cavity would have to be 14.7 GHz to simultaneously support both frequency modes, choosing a near-concentric design could still result in a small mode volume and thus in a high emission probability into a well-defined Gaussian mode. Alternatively, a fast π pulse together with the time-bin encoded qubit of the photon could be used [11]. Employing these techniques to increase the photon collection probability may dramatically increase the success probability of the gate and could make the generation of large entangled cluster states feasible.

We have demonstrated a probabilistic, heralded entanglement gate between two remote matter qubits with an average fidelity of $\bar{F} = 0.89(2)$. The remote entangling gate demonstrated here could be used to realize long-distance quantum repeaters and to demonstrate a loophole-free Bell-inequality violation. Furthermore, together with local operations, the entangling gate may be used to scalably generate cluster states for the realization of a one-way quantum computer [3–5,9,10].

This work is supported by the Intelligence Advanced Research Project Activity (IARPA) under Army Research Office contract, the National Science Foundation Physics at the Information Frontier program, and the NSF Physics Frontier Center at JQI.

*pmaunz@umd.edu

[1] D. Deutsch, Proc. R. Soc. A **425**, 73 (1989).
[2] R. Blatt and D. Wineland, Nature (London) **453**, 1008 (2008).
[3] H. J. Briegel and R. Raussendorf, Phys. Rev. Lett. **86**, 910 (2001).
[4] R. Raussendorf and H. J. Briegel, Phys. Rev. Lett. **86**, 5188 (2001).
[5] R. Raussendorf and H. J. Briegel, Quantum Inf. Comput. **2**, 443 (2002).
[6] P. Walther *et al.*, Nature (London) **434**, 169 (2005).
[7] C. Y. Lu *et al.*, Nature Phys. **3**, 91 (2007).
[8] T. P. Bodiya and L. M. Duan, Phys. Rev. Lett. **97**, 143601 (2006).
[9] L. M. Duan and R. Raussendorf, Phys. Rev. Lett. **95**, 080503 (2005).
[10] L. Duan *et al.*, Phys. Rev. A **73**, 062324 (2006).
[11] S. D. Barrett and P. Kok, Phys. Rev. A **71**, 060310 (2005).
[12] S. Olmschenk *et al.*, Science **323**, 486 (2009).
[13] D. J. Berkeland and M. G. Boshier, Phys. Rev. A **65**, 033413 (2002).
[14] P. Fisk *et al.*, IEEE Trans. Ultrason. Ferroelectr. Freq. Control **44**, 344 (1997).
[15] S. Olmschenk *et al.*, Phys. Rev. A **76**, 052314 (2007).
[16] M. J. Madsen *et al.*, Phys. Rev. Lett. **97**, 040505 (2006).
[17] C. K. Hong, Z. Y. Ou, and L. Mandel, Phys. Rev. Lett. **59**, 2044 (1987).
[18] Y. H. Shih and C. O. Alley, Phys. Rev. Lett. **61**, 2921 (1988).
[19] S. L. Braunstein and A. Mann, Phys. Rev. A **51**, R1727 (1995).
[20] C. Simon and W. T. M. Irvine, Phys. Rev. Lett. **91**, 110405 (2003).
[21] D. F. V. James *et al.*, Phys. Rev. A **64**, 052312 (2001).
[22] D. L. Moehring *et al.*, Nature (London) **449**, 68 (2007).
[23] D. N. Matsukevich *et al.*, Phys. Rev. Lett. **100**, 150404 (2008).
[24] R. Raussendorf and J. Harrington, Phys. Rev. Lett. **98**, 190504 (2007).
[25] N. Lindlein *et al.*, Laser Phys. **17**, 927 (2007).
[26] E. W. Streed *et al.*, arXiv:0805.2437.
[27] M. Hennrich *et al.*, Phys. Rev. Lett. **85**, 4872 (2000).
[28] J. McKeever *et al.*, Science **303**, 1992 (2004).